Available online at www.sciencedirect.com

ScienceDirect

Procedia CIRP 124 (2024) 291–294

www.elsevier.com/locate/procedia

13th CIRP Conference on Photonic Technologies [LANE 2024], 15-19 September 2024, Fürth, Germany

Spectral emission characteristics of single point exposure LPBF process

Ema Vasileska[a]*, Leonardo Caprio[b], Ali Gökhan Demir[b],

Vladimir Dukovski[a], Valentina Gecevska[a], Barbara Previtali[b]

[a]*Ss. Cyril and Methodius University in Skopje, Faculty of Mechanical Engineering - Skopje, Ruger Bosković 18, 1000 Skopje, North Macedonia;*
[b]*Politecnico di Milano, Department of Mechanical Engineering, Via La Masa 1, 20156 Milan, Italy*

* Corresponding author. Tel.: +38970204989. *E-mail address:* ema.vasileska@mf.edu.mk

Abstract

Despite the advantages of laser powder bed fusion (LPBF), part defects may arise from inaccurately chosen process parameters or heat accumulation during the scanning of complex geometries. Amongst different monitored entities the chemistry or the process fingerprints related to the material requires further attention. Monitoring the spectral content of light emitted from the laser-material interaction provides insight into thermal conditions and chemical composition of the processed material. This work implements an off-axial spectral monitoring setup for Optical Emission Spectroscopy (OES) in LPBF. Single-point experiment was conducted on AISI316L and Ti-6Al-4V. The study showed that the variation of laser energy input causes consequent variation of spectral emission intensity, as well as that the developed setup successfully captures spectral peaks of alloying elements. Principal Component Analysis demonstrated clear differentiation between the two materials. These findings prove the potential of OES for monitoring alloying elements of processed material and processing conditions in LPBF.

Keywords: laser powder bed fusion; optical emission spectroscopy; spectral emission monitoring.

1. Introduction

Laser powder bed fusion (LPBF) enables the fabrication of intricate lattice geometries and topologically optimized lightweight structures. However, these complex geometries often result in defects due to excessive energy input and heat accumulation, or improper parameter selection for the material, leading to porosity or lack of fusion [1]. One approach to address energy input in intricate geometries like lattice structures is through the scanning strategy. While continuous scanning is commonly used regardless of part geometry, recent research has leveraged the LPBF's precision and the small size of the laser beam to develop an alternative scan strategy called Single Point Exposure (SPE) [2]. This strategy offers greater control over temporal thermal accumulation, influencing melt pool behavior and solidification during lattice structure manufacturing. SPE consists in positioning of the laser beam at precise locations, which are then exposed to a single pulse with defined duration (t_{on}) and peak power (P), utilizing pulse wave (PW) modulation rather than continuous wave (CW). SPE has been previously applied in LPBF processes, notably reducing defects in critical part geometries for materials like Ti alloys and Zn-0.5 Mg [3], [4]. When using SPE, it is crucial to optimize the pulse parameters to balance melting dynamics, ensuring sufficient energy input for melting while preventing excessive vaporization.

Numerous monitoring methods are implemented in both off-axial and co-axial configuration, often utilizing cameras, photodiodes, and pyrometers [5]. However, limited attention has been given to Optical Emission Spectroscopy (OES). OES involves analyzing emitted light spectra during laser-material interaction, providing insights into chemical composition and elemental concentration near the melt pool as well as enabling temperature and electron density calculations in the vapor plume [6], [7], [8]. Monitoring each emission point during the SPE scanning can contribute to understanding of local

10.1016/j.procir.2024.08.120

processing dynamics and temperature distribution, facilitating observation of laser-material interaction and potential defect occurrence. Moreover, identifying materials being printed through peak analysis and intensity measurement in the emission spectrum enables automatic parameter selection and cross-contamination detection. While OES analysis has been utilized in laser welding and metal deposition to correlate quality factors and process parameters [9], [10], there are limited number of works for its application in LPBF [8], [11]. Photodiodes with band-pass filters to monitor elemental emission [12], plume temperature and melt pool size [13], and cross contaminations [14] have been analyzed, limiting the approach to the process condition.

This study introduces a spectral monitoring setup integrated into an LPBF machine, positioned off-axially to observe a fixed location on the powder bed. The feasibility of employing OES in LPBF is validated by acquiring and analyzing emission spectra during laser processing of two metal alloys using the single point exposure strategy for producing lattice struts.

2. Experiment methodology

2.1. Open LPBF platform

Experimental work was conducted on an open LPBF platform utilizing a single mode fiber laser (IPG Photonics YLR-300-AC-Y11, Cambridge, MA, USA), with a maximum power of 300W and an emission wavelength of 1070 nm. It is connected to a scanner head (AM Module v1.1, Raylase, Weßling, Germany) controlled with customized CAM software allowing flexibility in scan strategies (Direct Machining Control, Vilnius, Lithuania). Control and synchronization between mechanical movement and laser scanning are facilitated by a controller card (SP-ICE III, Raylase, Weßling, Germany), enabling customization of the hardware and software components for end-user accessibility.

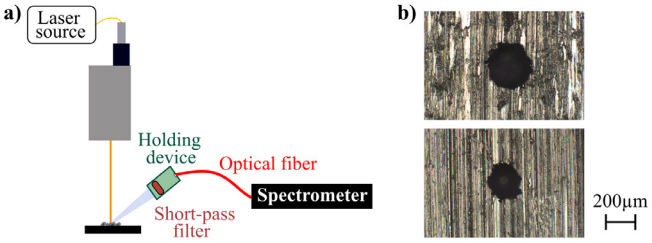

Fig. 1: a) Off-axial OES monitoring setup; b) Examples of SPE specimens attained with P=200W and t_{on}=800µs, on: (up) Ti-6Al-4V, (down) AISI316L

2.2. Off-axial spectral emission monitoring setup

A spectrometer with a 1200 lines/mm grating (Avantes 2048 USB2) was employed for spectrum acquisition throughout the experiments, covering a spectral range from 200 nm to 1100 nm (UV, VIS, and NIR). Throughout all experiments, the integration time was fixed at 10 ms to capture the process emission, exceeding the longest laser pulse duration used. Positioned off-axially approximately 250 mm from the powder bed, the monitoring sensor observed small region of interest on the powder bed where the interaction between laser and material occurs, as shown in Fig. 1 a). A short-pass filter (FESH1000, Thorlabs Inc, USA) was mounted before the optical fiber to block emission wavelengths above 1000 nm. Spectrometer acquisition was synchronized with the laser emission.

2.3. Experiment design

An experiment was conducted on the LPBF platform to assess the developed OES monitoring setup's suitability for LPBF processes. The experiment aimed to demonstrate the setup's capability to acquire spectra lines related to process emission; assess whether spectral line intensities vary with the delivered energy input; and determine if spectral peaks corresponding to alloying elements are detected. AISI316L and Ti-6Al-4V alloys were analyzed using the single point exposure LPBF strategy. Fixed and variable factors, along with their levels, are detailed in Table 1 for the full-factorial experiment with three repetitions.

Table 1: Fixed and variable factors in the experiment

Fixed factors	**Values**
Focal position, Δz [mm]	0
Powder layer height [µm]	50
Variable factors	**Values**
Material	AISI316L, Ti-6Al-4V
Laser power, P [W]	50-100-150-200
Laser exposure time, t_{on} [µs]	100-200-400-800

3. Results and discussion

3.1. Monitored emission spectrums as function of process parameters

Examples from SPE specimens on both materials attained with the highest energy input (P=200W and t_{on}=800µs) are presented in Fig. 1 b). The resulting spectral emissions of the examined materials are presented in Fig. 2 a) for AISI316L and in Fig. 2 b) for Ti-6Al-4V. These emission lines comprise both thermal effects and distinct spectral lines attributed to alloying elements. Spectral emission intensity varies noticeably as a function of laser power (P) and exposure time (t_{on}), increasing with the increase of energy input, particularly in the VIS and NIR wavelengths. Specific spectral peaks corresponding to alloying elements are visible in the emission spectra, serving as material fingerprints. Further details on these peaks are discussed in later subsection. The experiments demonstrated the statistically significant impact of t_{on} and P on emission intensity through analysis of variance (ANOVA), not reported here for the sake of brevity. The assessment of the mean and standard deviation of the signals has yielded P-values below the predefined significance threshold of 0.05, verifying the statistically significant influence of the process variables on the emission spectrum. These results indicate that employing an OES monitoring setup enables the observation of process dynamics influenced by variations in energetic input. The laser energy input during the process, defined by t_{on} and P, leads to diverse melting conditions in LPBF, giving rise to unwanted phenomena such as lack of fusion in instances of insufficient energy input, or keyholing porosity and overheating with excessive energy input, which in term result in defective part [15].

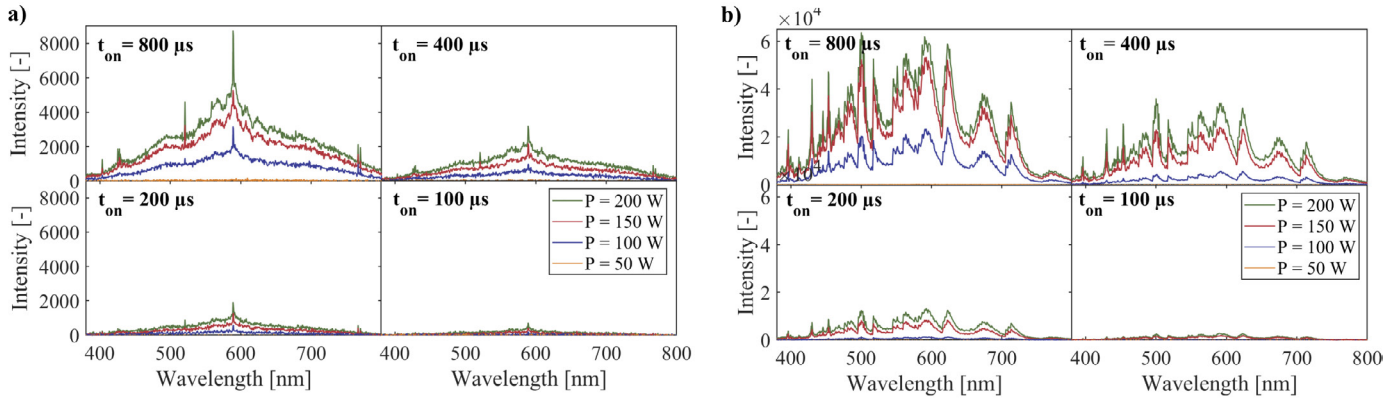

Fig. 2: Spectral emissions acquired with OES monitoring setup of: a) AISI316L; b) Ti-6Al-4V

Real-time OES monitoring of processing conditions and potential defects becomes feasible by examining emission intensities, allowing for corrective actions when observed faulty processing conditions. However, it is important to acknowledge that the effectiveness of real-time monitoring is constrained by the acquisition frequency of the sensor.

3.2. Spectral peaks related to alloying elements

Each element in the alloy is associated with spectral peak at a specific wavelength. Analysis was conducted to automatically identify and display relevant peaks in the spectra. This helps in assessing the repeatability of the monitoring setup across all spectra of the same material, as well as in comparing the wavelengths of the emission peaks with those of the alloying elements as defined by the atomic spectra database of National Institute of Standards and Technology (NIST) [16]. A peak detection algorithm was developed. The line of the raw emission signal is summing up the process thermal emission and the spectral lines. To isolate the emission lines along with their corresponding intensities, the thermal emission baseline was estimated and subtracted from the raw emission spectrum with the asymmetric least squares smoothing algorithm [17]. Following the subtraction of the baseline, only the emission peaks persist in the acquired spectrum, onward referred to as the subtracted spectrum. A peak detection algorithm was employed to identify local maximum points given a distance threshold and minimum height threshold. The outcomes are depicted in Fig. 3. On the figure the wavelengths of the detected peaks in the spectra obtained from the conducted experiments are illustrated. From these results, experiments that exhibited unmelted spots, resulting also with absence of a significant increase in the spectrum signal, were excluded from the study. Moreover, the figure presents an example subtracted spectrum in the wavelength range of 380 – 800 nm taken from the experiment with laser power equal to 200 W and exposure time equal to 800 µs, with appointed identified spectral peaks [16].

The developed spectral monitoring setup successfully captured the spectral peaks associated with the alloying elements. In the case of AISI316L, multiple peaks corresponding to the base element Fe were observed, along with peaks of Cr and Ni. For Ti-6Al-4V, peaks of Ti, the element with the highest concentration in the alloy, were evident, along with peaks of Al and V. It is evident that certain spectral peaks are not detected by the algorithm in some of the spectra, and in some cases, additional peaks emerge. This is especially observed when examining low-intensity peaks in AISI316L material. The peaks which are appearing in most experiments are aligned with the wavelengths corresponding to the alloying elements documented in the NIST database, thereby indicating the compositional characteristics of the metal alloy.

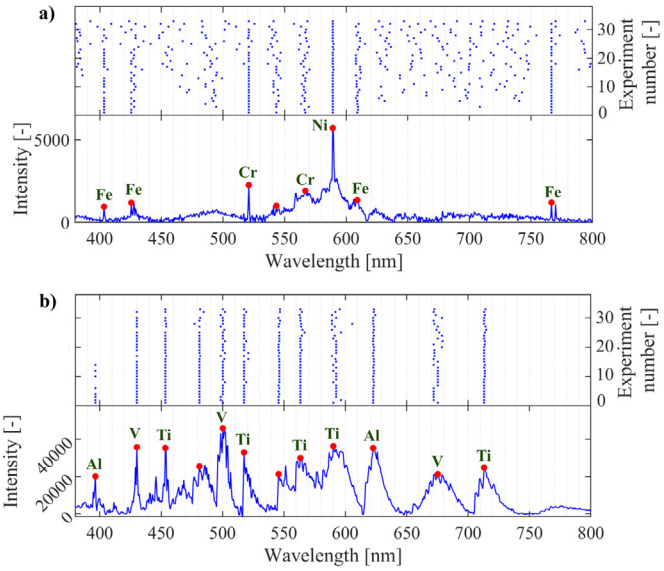

Fig. 3: Detected spectral peaks' wavelengths in the experiments and the subtracted spectrum from the experiment with P=200W and ton=800µs, showcasing identified spectral lines, for: a) AISI316L; b) Ti-6Al-4V.

Peaks that are not detected in most experiments may indicate the presence of alloying elements in the material or could potentially be attributed to noise introduced by the peak detection algorithm. Regardless, the recurrent appearance of peaks establishes a foundation for subsequent analyses at specific spectral wavelengths aimed at monitoring process conditions, which can be utilized for material identification. As a first step toward this purpose, principal component analysis (PCA) was conducted using the entire spectral emission profile

after the removal of the thermal profile. The results are shown in Fig. 4. The first two principal components were utilized since they account for approximately 99.7 % of the variability within the input emission data. The high explanatory capacity of these two components underscores their effectiveness in summarizing critical spectral information. The score plot generated using the first two principal components revealed clear differentiation between the materials, as evidenced by the distinct clusters that represent the two materials. This outcome underscores the utility of PCA as a robust analytical tool for material identification within intricate spectral datasets.

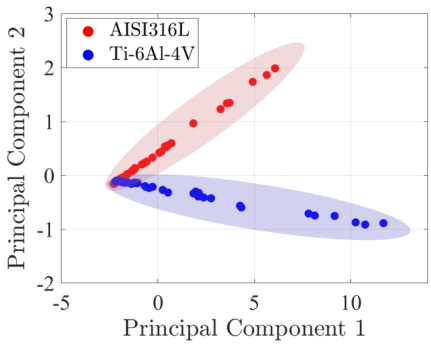

Fig. 4: Score plot of first two principal components grouping the two materials

4. Conclusions

The work presents the development and implementation of off-axial spectral monitoring setup on LPBF machine viewing a fixed position on the powder bed. A full-factorial single point exposure experiment validated the applicability of spectral emission monitoring in LPBF, using AISI316L and Ti-6Al-4V alloys. Key findings include:

- Monitoring of spectral emission in the LPBF process is feasible in the processing atmosphere;
- The variation of laser energy input incites consequent variation of the spectral emission intensity;
- After subtracting the thermal effects, identification of alloying element spectral lines was possible, thus providing means for material identification;
- PCA showed precise clustering of the two materials when the first two principal components are used.

These results affirm the potential of OES in LPBF for monitoring alloying elements and processing conditions via emission intensity. The off-axial setup, while effective, has limitations such as a fixed observational region. Future research will focus on designing and implementing a coaxial OES setup for real-time process monitoring.

References

[1] E. Vasileska, A. G. Demir, B. M. Colosimo, and B. Previtali, “A novel paradigm for feedback control in LPBF: layer-wise correction for overhang structures,” *Adv Manuf*, vol. 10, no. 2, pp. 326–344, 2022, doi: 10.1007/s40436-021-00379-6.

[2] L. Caprio, F. Guaglione, and A.G. Demir, “Development of Single Point Exposure Strategy to Suppress Vapour Formation During the Laser Powder Bed Fusion of Zinc and Its Alloys,” In: Carrino, L., Tolio, T. (eds) *Selected Topics in Manufacturing. Lecture Notes in Mechanical Engineering*, Springer, 2022, doi: 10.1007/978-3-030-82627-7_7.

[3] E. Onal, A. E. Medvedev, M. A. Leeflang, A. Molotnikov, and A. A. Zadpoor, “Novel microstructural features of selective laser melted lattice struts fabricated with single point exposure scanning,” *Addit Manuf*, vol. 29, p. 100785, 2019, doi: 10.1016/j.addma.2019.100785.

[4] F. Guaglione, L. Caprio, B. Previtali, and A. G. Demir, “Single point exposure LPBF for the production of biodegradable Zn-alloy lattice structures,” *Addit Manuf*, vol. 48, no. October, 2021, doi: 10.1016/j.addma.2021.102426.

[5] M. Grasso, A. Remani, A. Dickins, B. Colosimo, and R. Leach, “In-situ measurement and monitoring methods for metal powder bed fusion: An updated review,” *Meas Sci Technol*, vol. 32, Jul. 2021, doi: 10.1088/1361-6501/ac0b6b.

[6] Y. Kawahito, N. Matsumoto, M. Mizutani, and S. Katayama, “Characterisation of plasma induced during high power fibre laser welding of stainless steel,” *Science and Technology of Welding and Joining*, vol. 13, no. 8, pp. 744–748, Nov. 2008, doi: 10.1179/136217108X329313.

[7] M. Collur and T. Debroy, “Emission spectroscopy of plasma during laser welding of AISI 201 stainless steel,” *Metallurgical transactions. B, Process metallurgy*, vol. 20, pp. 277–286, Apr. 1989, doi: 10.1007/BF02825608.

[8] A. R. Ziefuss, R. Streubel, P. Gabriel, F. Eibl, and S. Barcikowski, “In-situ monitoring of the material composition in PBF-LB via optical emission spectroscopy.” *ChemRxiv*, 2023, doi: 10.26434/chemrxiv-2023-m977f. *This content is a preprint and has not been peer-reviewed.*

[9] L. Song and J. Mazumder, “Real Time Cr Measurement Using Optical Emission Spectroscopy During Direct Metal Deposition Process,” *IEEE Sens J*, vol. 12, no. 5, pp. 958–964, 2012, doi: 10.1109/JSEN.2011.2162316.

[10] A. R. Nassar, T. J. Spurgeon, and E. W. Reutzel, “Sensing defects during directed-energy additive manufacturing of metal parts using optical emissions spectroscopy,” *2014 International Solid Freeform Fabrication Symposium*, 2014, doi: 10.26153/tsw/15684.

[11] A. J. Dunbar, A. R. Nassar, E. W. Reutzel, and J. J. Blecher, “A real-time communication architecture for metal powder bed fusion additive manufacturing,” *Solid Freeform Fabrication 2016: Proceedings of the 27th Annual International Solid Freeform Fabrication Symposium - An Additive Manufacturing Conference,* 2016, pp. 67–80, 2016.

[12] A. J. Dunbar and A. R. Nassar, “Assessment of optical emission analysis for in-process monitoring of powder bed fusion additive manufacturing,” *Virtual Phys Prototyp*, vol. 13, no. 1, pp. 14–19, Jan. 2018, doi: 10.1080/17452759.2017.1392683.

[13] C. S. Lough *et al.*, “In-situ optical emission spectroscopy of selective laser melting,” *J Manuf Process*, vol. 53, pp. 336–341, 2020, doi: 10.1016/j.jmapro.2020.02.016.

[14] M. Montazeri, R. Yavari, P. Rao, and P. Boulware, “In-Process Monitoring of Material Cross-Contamination Defects in Laser Powder Bed Fusion,” *J Manuf Sci Eng*, vol. 140, no. 11, 2018, doi: 10.1115/1.4040543.

[15] E. Vasileska, A. G. Demir, B. M. Colosimo, and B. Previtali, “Layer-wise control of selective laser melting by means of inline melt pool area measurements,” *J. Laser Appl.*, vol. 32, no. 022057, 2020, doi: 10.2351/7.0000108.

[16] “NIST Atomic Spectra Database,” https://www.nist.gov/pml/atomic-spectra-database.

[17] P. Eilers and H. Boelens, “Baseline Correction with Asymmetric Least Squares Smoothing,” *LeidenUniversity Medical Centre Report 1*, vol. 5, Nov. 2005.